energies

Article

Non-Symmetrical (NS) Reconfiguration Techniques to Enhance Power Generation Capability of Solar PV System

Suresh Mikkili [1,*], Akshay Kanjune [1], Praveen Kumar Bonthagorla [1] and Tomonobu Senjyu [2,*]

[1] Department of Electrical and Electronics Engineering, National Institute of Technology Goa, Ponda 403401, India; akshayk2223@gmail.com (A.K.); praveennitgoa2017@gmail.com (P.K.B.)
[2] Department of Electrical and Electronics Engineering, Faculty of Engineering, University of the Ryukyus, Okinawa 903-0213, Japan
* Correspondence: mikkili.suresh@nitgoa.ac.in (S.M.); b985542@tec.u-ryukyu.ac.jp (T.S.)

Abstract: At present, primary power generation depends on non-renewable energy resources, which will become extinct. Solar is the best option in renewable energy sources to achieve clean and green power extraction. Solar PV transforms light energy into electrical energy. However, the output power of solar PV changes with solar insolation. It is also affected by environmental factors and the shading effect. One of the key factors that can reduce the PV system output power is partial shading condition (PSC). The reduction in power output not only depends on shaded region but also depends on pattern of shading and physical position of shaded modules in the array. Due to PSCs, mismatch losses are induced between the shaded modules which can cause several peaks in the output power-voltage (P-V) characteristic. This article describes the non-symmetrical reconfiguration technique and compares it with the primary total cross tied connection. The performance of non-symmetrical reconfiguration techniques is evaluated and compared in terms of global maximum power (GMP), voltage and currents at GMP, open and short circuit voltage and currents, mismatch power loss (MPL), fill factor, efficiency, and number of local maximum power peaks (LMPPs) on a 9×9 PV array.

Keywords: non-symmetrical (NS) reconfiguration techniques; total cross tied (TCT); global maximum power point (GMPP); mismatch loss (ML)

check for updates

Citation: Mikkili, S.; Kanjune, A.; Bonthagorla, P.K.; Senjyu, T. Non-Symmetrical (NS) Reconfiguration Techniques to Enhance Power Generation Capability of Solar PV System. *Energies* **2022**, *15*, 2124. https://doi.org/10.3390/en15062124

Academic Editors: Wei-Hsin Chen, Aristotle T. Ubando, Chih-Che Chueh, Liwen Jin, Alon Kuperman and Akhtar Kalam

Received: 23 January 2022
Accepted: 8 March 2022
Published: 14 March 2022

Publisher's Note: MDPI stays neutral with regard to jurisdictional claims in published maps and institutional affiliations.

Copyright: © 2022 by the authors. Licensee MDPI, Basel, Switzerland. This article is an open access article distributed under the terms and conditions of the Creative Commons Attribution (CC BY) license (https://creativecommons.org/licenses/by/4.0/).

1. Introduction

Electricity is one of the crucial factors in the development of a nation. Due to the growing population and energy demand, the whole world is facing a problem of energy deficiency [1]. Electricity demand has had the fastest growth in the last 10 years. The global energy demand will increase by 4.6% in 2021 [2]. In October 2021, India recorded a power shortage of 1201 million units due to a lack of coal. The coal demand is increased by 4.5% in 2021 [3,4]. The use of renewable resources reduces coal dependency and pollution. India shares the second largest renewable energy generation globally after China. Solar energy's abundant, free availability, and eco-friendly nature increase its share in the energy sector. The power generation of the PV array is dependent on various factors such as irradiance, temperature, configuration, environmental factors, etc. [5]. Shading cases such as trees, neighboring buildings, soiling, ice accumulation, etc., reduces PV array power generation [6]. Reconfiguration enhances the power generation of PV arrays [7]. This paper proposes a non-symmetrical (NS) reconfiguration technique to enhance the solar PV system power generation capability on a 9×9 PV array under six partial shading conditions.

2. Literature Survey

2.1. Solar Energy Perspective in India

The Indian grid has five regions: north, east, west, south, and northeast. To achieve the goal of 'one-nation-one-grid,' all these regions are connected, forming one grid. India is a tropical country. It receives a large amount of solar energy [8]. In India, there are three categories of solar power plants: Small (range less than 99 megawatts (MW)), Medium (from 100 to 400 MW), and Large (greater than 400 MW) [9]. The Government of India launched a program of National Solar Mission. In recent years, there has been a significant development in renewable energy uses. Initially, India aimed to achieve 100 GW of solar energy by 2022 [10]. Most of the electricity has generated from the thermal power plant. This thermal power plant has various demerits. The coal used for combustion purposes created the carbon emissions problem. Additionally, the by-product (ash) handling issues are there as it requires a large amount of land for ash storage in nuclear power plants. Atomic fuels have been used for the combustion in these plants. This atomic fuel is hazardous to living things. Nuclear waste is radioactive. The advantages of utilizing renewable resources are listed as below:

1. Clean power: renewable energy generates clean power as it does not create greenhouse gases and any other radioactive waste.
2. Economical: without financial help, onshore wind and solar PV electricity are usually less expensive than any fossil fuel option. Renewables are the competitive backbone of energy decarburization due to low and dropping technical prices.
3. Reduction in dependency of raw materials (fuels) for energy generation: renewable energy is available free of cost and in vast amounts.

Therefore, the generation of power from renewable resources causes a reduction in dependency on raw materials (fuels) for energy generation.

A solar electric vehicle is a vehicle powered by using solar energy. Using solar energy to generate electricity reduces the drawback of conventional energy generation techniques. Solar PV installed on a rooftop can provide power to isolated grid sections and remote places. Therefore, this helps reduce smoke from vehicles [11].

2.2. Factors Affecting the Performance of Solar Photovoltaic Systems

The factors affecting the solar photovoltaic output power and efficiency are as follows [12–15]:

- Degradation of the solar module: the module guarantees that the average life of the module is 25 years, but after some time, it starts degrading, and the output power gets reduced [12].
- Parasitic resistance: the series and shunt resistance of solar PV called parasitic resistance causes power loss in solar PV [13].
- Temperature: the performance of solar cells degrades as the temperature rises. Internal carrier recombination rates have grown due to higher carrier concentrations [13].
- Shadow: shading causes mismatches in the current generated between individual cells, which will cause the cell to get damaged due to heating [14].
- Maintenance: dust and dirt cause a reduction in the output power of solar PV.
- Dynamic solar radiation: continuous varying solar radiation causes an effect on solar PV [15].
- Solar panel conversion loss: the solar PV converts light energy into electrical energy. The considerable and best efficiency of solar PV available is in the range of 18–24%.
- Inverter and battery efficiency: in a PV system, the efficiency of the string inverter is about 97%. The batteries have an efficiency of about 85%, which has a 5–15%—conversion loss in a storm [16].
- Conductor power loss/transfer loss: the cable used for carrying current has some resistance. Due to this, there is power loss, i.e., I^2R loss, which has dissipated in the form of heat [17].

The above factors, environmental condition, type and time of shadow, connection structure, system working losses, etc., are many more factors. Therefore, to enhance the power, reconfiguration techniques are one of the best solutions [7].

2.3. Configuration and Reconfiguration Techniques

PV panels have been connected in series, parallel, series-parallel, TCT, H-C, and B-L to generate the required power generation. TCT has the best performance among them [18]. The TCT setup, on the other hand, has the effect of partial shading, lowering the output power. Ref. [19] gives various hybrid connections such as BL-TCT and reconfigured conventional configurations. Ref. [20] proposes a screw pattern array configuration scheme for a 9 × 9 PV array. Ref. [21] suggests a triple tide connection to enhance the power extraction. Many authors have utilized different reconfiguration strategies to reduce the downside of the TCT configuration under partial shading conditions. Physically shifting the solar PV to retain the electrical connection or alternating electrical connection keeping the physical position constant are also examples of reconfiguration. Changing the panel from its location is called static reconfiguration. Changing the electrical connection of the PV panel is called dynamic reconfiguration [22].

Ref. [23] has presented an adaptive reconfiguration mode to lower the influence of shadows on solar panels. A switch matrix is used in model-based control to connect an adaptive solar bank to a fixed area of the photovoltaic array, boosting the array's power production. Ref. [24] proposed a dynamic electric array reconfiguration concept based on a switching matrix topology to boost energy output. Ref. [25] proposes dynamic reconfiguration, which propagates in an L shape to reconfigure the array structure. Various static and dynamic reconfiguration solutions are investigated in [26] to reduce power losses induced by partial shadow. Due to the cost and complexity, many researchers have contributed to physical array reconfiguration. In static repositioning, panels can be repositioned either at any location of an array or limited to the same column [27–29]. Ref. [30] proposes a magic square technique with a 9 × 9 PV array structure to improve the power output. Ref. [31] proposes a novel magic square. Ref. [32] proposes a skyscraper puzzle, based methods. Ref. [33] gives a two-phase reconfiguration method. However, the above-mentioned methods have a limitation of PV panel sizing.

This article proposes simple, reliable, and practical, non-symmetrical static reconfiguration techniques to enhance the power from PV panels under shading conditions. Here, the panel location has changed logically to mitigate the shadowing effects. Matlab/simulation with a 170 W PV panel was completed on a 9 × 9 array structure. The complete technical details of PV panels are given in Section 6. The electrical connections were made per the TCT connection to develop proposed methods. A 9 × 9 TCT model is shown in Figure 1.

11	12	13	14	15	16	17	18	19
21	22	23	24	25	26	27	28	29
31	32	33	34	35	36	37	38	39
41	42	43	44	45	46	47	48	49
51	52	53	54	55	56	57	58	59
61	62	63	64	65	66	67	68	69
71	72	73	74	75	76	77	78	79
81	82	83	84	85	86	87	88	89
91	92	93	94	95	96	97	98	99

Figure 1. Total cross-tied 9 × 9 array.

3. Non-Symmetrical (NS) Reconfiguration Technique

The rows were interchanged in a non-symmetrical pattern, and the column was kept the same. The row should be an odd number to obtain the two different non-symmetrical configuration arrangements. Otherwise, only one non-symmetrical structure is possible for an even number of rows. The rules for forming a non-symmetrical pattern are described below. Consider a PV panel A_{xy}, X represents row number and y represents column number.

3.1. Algorithm/Rule for Non-Symmetrical Arrangement-1

The implementation of Non-Symmetrical Arrangement-1 based reconfiguration algorithm is given in Algorithm 1.

Algorithm 1. Algorithm for Non-Symmetrical Arrangement-1.

$$x = \begin{cases} x & ,if\ y = 1 \\ x + (y-1)floor(x_{max}/2) & ,\ if\ y > 1 \end{cases}$$
if $\quad x \leq x_{max}\ , x = x$
else $\quad x = x - x_{max}$

Explanation: For the NS-1 arrangement, the floor was considered. Floor means the smallest and closest whole number to the integer, i.e.,$x_{max}/2$. Consider column two. In column two, i.e., y = 2 for row x = 4 then value of row as per NS-1 algorithm will be

$$\begin{aligned} \mathrm{x} &= \mathrm{x} + (\mathrm{y} - 1)\ 8{*}\mathrm{floor}(\mathrm{x}_{\max}/2) \\ \mathrm{x} &= 4 + (2-1){*}\ \mathrm{floor}(9/2) \\ \mathrm{x} &= 4 + (1){*}\ \mathrm{floor}(4.5) \end{aligned}$$

since, $\mathrm{floor}(4.5) = 4$, $\mathrm{x} = 4 + 4$

$$\mathrm{x} = 8$$

Similarly, considering the above algorithm in the same column two y = 2, if row six x = 6 is considered, then the value of the row as per the NS-1 algorithm will be

$$\begin{aligned} \mathrm{x} &= \mathrm{x} + (\mathrm{y} - 1)\ 8{*}\mathrm{floor}(\mathrm{x}_{\max}/2) \\ \mathrm{x} &= 6 + (2-1){*}\ \mathrm{floor}(9/2) \\ \mathrm{x} &= 6 + (1){*}\ \mathrm{floor}(4.5) \end{aligned}$$

since, $\mathrm{floor}\ (4.5) = 4$, $\mathrm{x} = 6 + 4$

$$\mathrm{x} = 10$$

Here, $\mathrm{x} > \mathrm{x}_{\max}$ then value of x will be,

$$\begin{aligned} \mathrm{x} &= \mathrm{x} - \mathrm{x}_{\max} \\ \mathrm{x} &= 10 - 9 = 1 \end{aligned}$$

Similar to this, the whole 9 × 9 array was formed using the NS-1 rule. In this non-symmetrical-1 reconfiguration method, only the row number of the PV panel has changed, but the column has not changed.

3.2. Algorithm/Rule for Non-Symmetrical Arrangement-2

The implementation of Non-Symmetrical Arrangement-2 based reconfiguration algorithm is given in Algorithm 2.

Algorithm 2. Algorithm for Non-Symmetrical Arrangement-2.

$$\mathrm{x} = \begin{cases} \mathrm{x} & , \quad \text{if } \mathrm{y} = 1 \\ \mathrm{x} + \mathrm{ceil}(\mathrm{x}_{\max}/2) & , \quad \text{if } \mathrm{y} > 1 \end{cases}$$
if $\quad \mathrm{x} \leq \mathrm{x}_{\max}\ , \mathrm{x} = \mathrm{x}$
else $\quad \mathrm{x} = \mathrm{x} - \mathrm{x}_{\max}$

Explanation: For NS-2 arrangement, ceil was considered. Ceil means the bigger and closest whole number to the integer, i.e., $x_{max}/2$. Consider column two. In column two, i.e., y = 2 for row x = 4 then the value of the row as per the NS-2 algorithm will be

$$x = x + (y - 1)\ 8{*}\mathrm{ceil}(x_{max}/2)$$
$$x = 4 + (2 - 1){*}\ \mathrm{ceil}(9/2)$$
$$x = 4 + (1){*}\ \mathrm{ceil}(4.5)$$

since ceil $(4.5) = 5$, $x = 4 + 5$

$$x = 9$$

Similarly, considering the above algorithm in the same column two y = 2, if row five x = 5, the row value as per the NS-2 algorithm will be

$$x = x + (y - 1)\ 8{*}\mathrm{ceil}(x_{max}/2)$$
$$x = 5 + (2 - 1){*}\ \mathrm{ceil}(9/2)$$
$$x = 5 + (1){*}\ \mathrm{ceil}(4.5)$$

since $\mathrm{ceil}(4.5) = 5$, $x = 5 + 5$

$$x = 10$$

Here, $x > x_{max}$ then value of x will be

$$x = x - x_{max}$$
$$x = 10 - 9 = 2$$

By using the NS-2 rule, the whole 9 × 9 array was formed. In this non-symmetrical-2 reconfiguration method, only the row number of the PV panel has changed, but the column has not changed.

Table 1 shows the values of floor and ceil for different x_{max}. Table 2 shows the pattern for the 9 × 9 array formed by using rules of non-symmetrical-1. Table 3 shows the 9 × 9 array formed by using the rules of non-symmetrical-2 techniques. Figure 2 shows a flow chart of non-symmetrical-1. Figure 3 shows the non-symmetrical-1 pattern. Figure 4 shows the non-symmetrical-2 arrangement 9 × 9 array. Figure 5 shows the flow chart of non-symmetrical-2. Figure 6 shows the non-symmetrical-2 way. Figure 7 shows the non-symmetrical-2 structure 9 × 9 array.

Table 1. Values of floor and ceil for different x_{max}.

x_{max}	*ceil* $(x_{max}/2)$	*floor* $(x_{max}/2)$
3	2	1
5	3	2
7	4	3
9	5	4

Table 2. Non-symmetrical arrangement-1 for PV array 9 × 9.

Column 1	**Column 2 =**	**Column 3 =**	**Column 4 =**	**Column 5 =**	**Column 6 =**	**Column 7 =**	**Column 8 =**	**Column 9 =**
Column 1	**Column 1 + 4**	**Column 2 + 4**	**Column 3 + 4**	**Column 4 + 4**	**Column 5 + 4**	**Column 6 + 4**	**Column 7 + 4**	**Column 8 + 4**
1	5	9	13 − 9 = 4	8	12 − 9 = 3	7	11 − 9 = 2	6
2	6	10 − 9 = 1	5	9	13 − 9 = 4	8	12 − 9 = 3	7
3	7	11 − 9 = 2	6	10 − 9 = 1	5	9	13 − 9 = 4	8
4	8	12 − 9 = 3	7	11 − 9 = 2	6	10 − 9 = 1	5	9
5	9	13 − 9 = 4	8	12 − 9 = 3	7	11-9 = 2	6	10 − 9 = 1
6	10 − 9 = 1	5	9	13 − 9 = 4	8	12 − 9 = 3	7	11 − 9 = 2
7	11 − 9 = 2	6	10 − 9 = 1	5	9	13 − 9 = 4	8	12 − 9 = 3
8	12 − 9 = 3	7	11 − 9 = 2	6	10 − 9 = 1	5	9	13 − 9 = 4
9	13 − 9 = 4	8	12 − 9 = 3	7	11 − 9 = 2	6	10 − 9 = 1	5

Table 3. Non-symmetrical arrangement-2 for PV array 9 × 9.

Column 1	Column 2 =	Column 3 =	Column 4 =	Column 5 =	Column 6 =	Column 7 =	Column 8 =	Column 9 =
Column 1	Column 1 + 4	Column 2 + 4	Column 3 + 4	Column 4 + 4	Column 5 + 4	Column 6 + 4	Column 7 + 4	Column 8 + 4
1	6	11 − 9 = 2	7	12 − 9 = 3	8	13 − 9 = 4	9	14 − 9 = 5
2	7	12 − 9 = 3	8	13 − 9 = 4	9	14 − 9 = 5	10 − 9 = 1	6
3	8	13 − 9 = 4	9	14 − 9 = 5	10 − 9 = 1	6	11 − 9 = 2	7
4	9	14 − 9 = 5	10 − 9 = 1	6	11 − 9 = 2	7	12 − 9 = 3	8
5	10 − 9 = 1	15 − 9 = 6	11 − 9 = 2	7	12 − 9 = 3	8	13 − 9 = 4	9
6	11 − 9 = 2	7	12 − 9 = 3	8	13 − 9 = 4	9	14 − 9 = 5	10 − 9 = 1
7	12 − 9 = 3	8	13 − 9 = 4	9	14 − 9 = 5	10 − 9 = 1	6	11 − 9 = 2
8	13 − 9 = 4	9	14 − 9 = 5	10 − 9 = 1	6	11 − 9 = 2	7	12 − 9 = 3
9	14 − 9 = 5	10 − 9 = 1	6	11 − 9 = 2	7	12 − 9 = 3	8	13 − 9 = 4

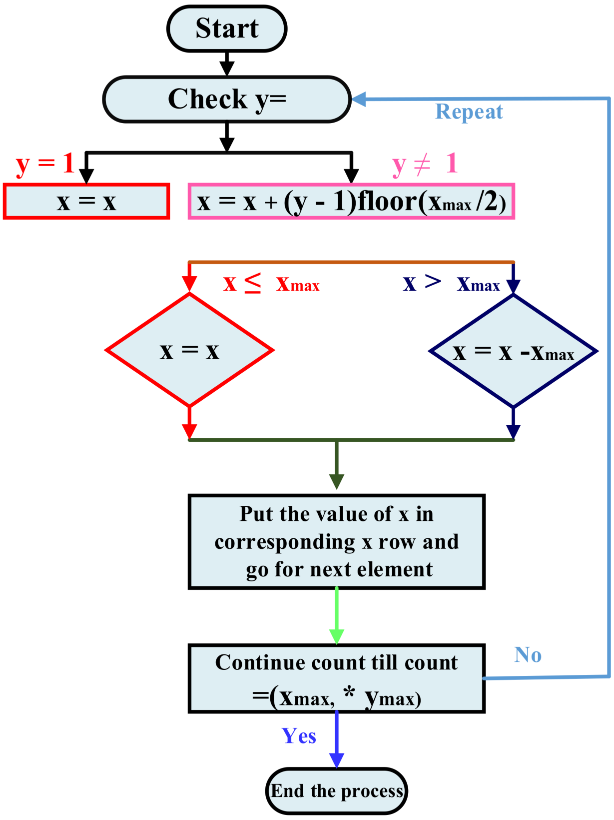

Figure 2. Flowchart of non-symmetrical-1, the x_{max} * y_{max} denotes the size of the matrix.

1	5	9	4	8	3	7	2	6
2	6	1	5	9	4	8	3	7
3	7	2	6	1	5	9	4	8
4	8	3	7	2	6	1	5	9
5	9	4	8	3	7	2	6	1
6	1	5	9	4	8	3	7	2
7	2	6	1	5	9	4	8	3
8	3	7	2	6	1	5	9	4
9	4	8	3	7	2	6	1	5

Figure 3. Non-symmetrical-1 pattern.

11	52	93	44	85	36	77	28	69
21	62	13	54	95	46	87	38	79
31	72	23	64	15	56	97	48	89
41	82	33	74	25	66	17	58	99
51	92	43	84	35	76	27	68	19
61	12	53	94	45	86	37	78	29
71	22	63	14	55	96	47	88	39
81	32	73	24	65	16	57	98	49
91	42	83	34	75	26	67	18	59

Figure 4. Symmetrical-1 array.

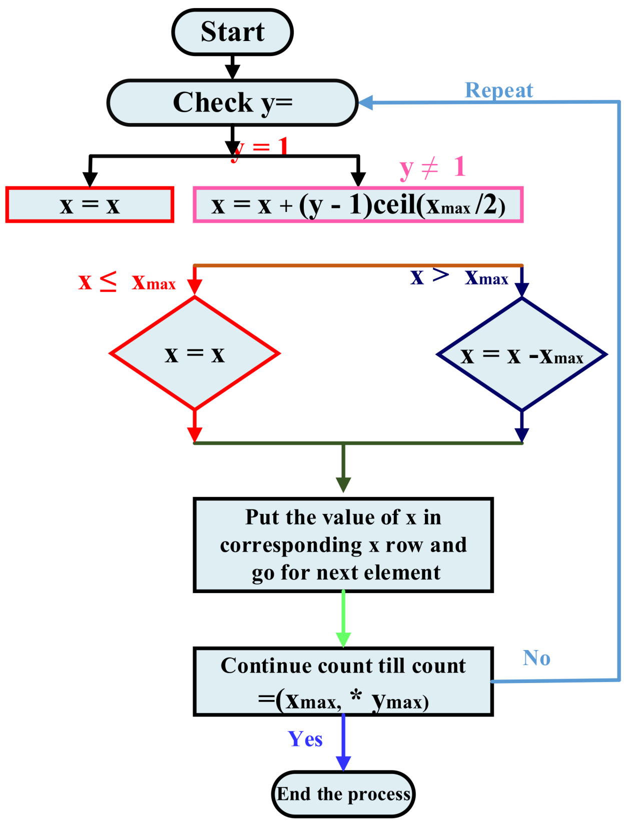

Figure 5. Flowchart of symmetrical-2, the x_{max} * y_{max} denotes the size of the matrix.

Therefore, the merits of the non-symmetrical reconfiguration technique are:

- It increases the power generated, FF, and efficiency.
- Power loss due to shading gets reduced as compared to the TCT configuration.
- It does not require any switching matrix such as the dynamic reconfiguration technique and relative losses.
- It reduces the local multiple power peaks in the PV curve and smoothens the PV curve.

Additionally, the only limitations are:

- Additional cable power loss due to cable and requirement of a skilled person.

1	6	2	7	3	8	4	9	5
2	7	3	8	4	9	5	1	6
3	8	4	9	5	1	6	2	7
4	9	5	1	6	2	7	3	8
5	1	6	2	7	3	8	4	9
6	2	7	3	8	4	9	5	1
7	3	8	4	9	5	1	6	2
8	4	9	5	1	6	5	7	3
9	5	1	6	2	7	3	8	4

Figure 6. Non-symmetrical-2 pattern.

11	62	23	74	35	86	47	98	59
21	72	33	84	45	96	57	18	69
31	82	43	94	55	16	67	28	79
41	92	53	14	65	26	77	38	89
51	12	63	24	75	36	87	48	99
61	22	73	34	85	46	97	58	19
71	32	83	44	95	56	17	68	29
81	42	93	54	15	66	27	78	39
91	52	13	64	25	76	37	88	49

Figure 7. Non-symmetrical-2 array.

4. Results and Discussion

This section discusses the MATLAB simulation results of the non-symmetrical reconfiguration technique under six different shading conditions. The considered shading conditions are Bottom of Right Corner (BORC), Bottom of Left Corner (BOLC), Top of Right Corner (TORC), Top of Left Corner (TOLC), and Centre (C) In these PSCs, five cases have shade on the 4 × 4 matrix, and the last one has shade on two sub-arrays of the 3 × 3 matrix. The shading has a 4 × 4 size in the first five shading conditions. This section compares basic connection techniques, total-cross-tied and non-symmetrical under the shading condition. Based on various factors, such as V_{OC} in volts (V), I_{SC} in amperes (A), GMPP in watts (W), V_{GMPP} in Volts (V), I_{GMPP} in amperes (A), % power loss and % fill factor, their performance was compared.

4.1. Normal Shading Condition

Under normal shading conditions, all solar PV receives a uniform solar insolation level, i.e., 1000 W/m^2. As mentioned in Table 4, various parameters were observed for this normal shading condition.

Table 4. Parameters under normal shading condition in the total cross tied arrangement.

V_{OC} (Volts)	I_{SC} (Ampere)	GMPP (Watt)	V_{GMPP} (Volts)	I_{GMPP} (Ampere)
397.8	46.9539	13,773	321.4876	42.8414

4.2. First: BORC 4 × 4 Sub-Array Shading Condition

BORC means the bottom of the right corner 4 × 4 sub-array. In this shading effect, parameters were compared between total cross tied, non-symmetrical-1, and non-symmetrical-2. Various parameters were compared between these three, such as ML, FF, and η. Figure 8 shows the BORC shading for (a) total cross tied arrangement (b) solar insolation levels (SIL), (c) NS-1 arrangement, (d) shading dispersion (SD) in NS-1, (e) NS-2 arrangement, (f) shading dispersion (SD) in NS-2. In Table 5, a comparison of TCT, NS-1, and NS-2 parameters is provided. From the same Table 5, it is evident that FF for NS-1 and NS-2 is 71.3935% and 70.3517%, respectively, whereas, for TCT, it is 62.4231%. The NS-1 and NS-2 have ML of 7.8196% and 9.3443%, respectively, and for TCT it is 15.7409%. The power enhanced by NS-1 is 9.4011%, and NS-2 is 7.59% compared to the total cross tied configuration under BORC shading for a 4 × 4 sub-array. Figure 9 shows the power-voltage (P-V) characteristic for BORC shading for a 4 × 4 sub-array and uniform shading condition. This characteristic represents the P-V curve for TCT under normal shading conditions, TCT under partial shading conditions, NS-1 and NS-2 under shading conditions. The PV curve shows that this NS-1 has the highest GMPP point under this shading condition, followed by NS-2 and TCT.

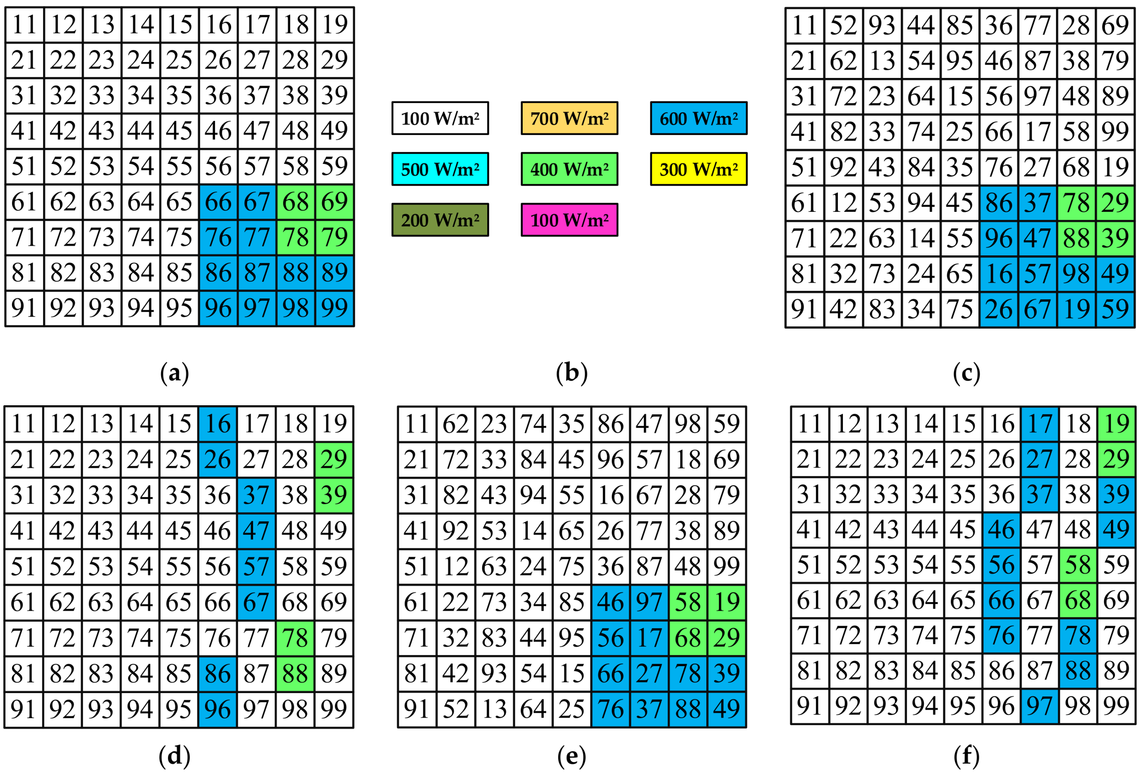

Figure 8. BORC 4 × 4 subarray shading for a 9 × 9 array. (**a**) Total cross tied arrangement, (**b**) solar insolation levels (SIL), (**c**) NS-1 arrangement, (**d**) shading dispersion (SD) in NS-1, (**e**) NS-2 arrangement, (**f**) shading dispersion (SD) in NS-2.

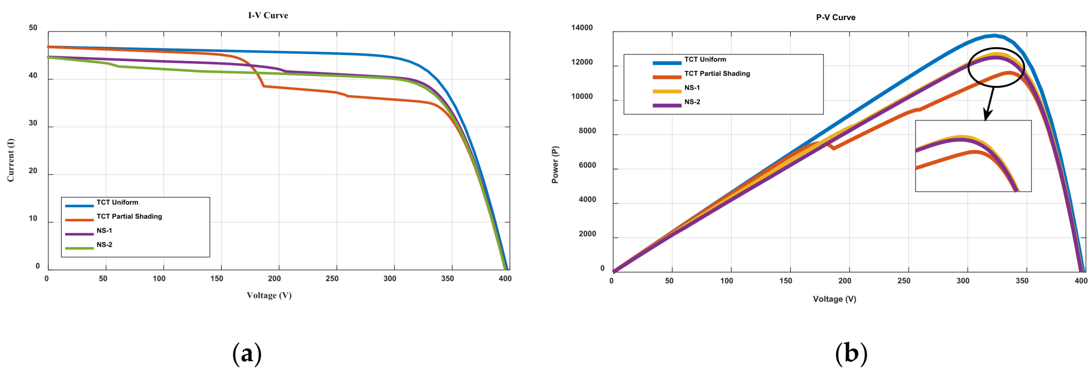

Figure 9. (**a**) I-V curve, (**b**) P-V curve, for BORC 4 × 4 subarray and uniform shading.

Table 5. Comparison between total cross tied, NS-1, and NS-2 arrangements under BORC 4 × 4 sub-array shading condition.

Method	V_{OC} (Volts)	I_{SC} (Ampere)	GMPP (Watt)	I_{GMPP} (Ampere)	V_{GMPP} (Volts)	% Power Loss	% Fill Factor
TCT	396.0500	46.9407	11,605	34.8333	335.3143	15.7409	62.4231
NS1	396.4674	44.8539	12,696	38.9835	325.6884	7.8196	71.3935
NS2	396.075	44.8096	12,486	38.3018	325.9793	9.3443	70.3517

4.3. Second: BOLC 4 × 4 Sub-Array Shading Condition

BOLC means Bottom of Left Corner 4 × 4 sub-array. In this shading effect, a performance comparison was made between total cross tied, non-symmetrical-1, and non-symmetrical-2. Various parameters were compared between these three, such as ML, FF, and η. Figure 10 shows the BOLC 4 × 4 sub-array shading for (a) total cross tied arrangement, (b) solar insolation levels (SIL), (c) NS-1 arrangement, (d) shading dispersion (SD) in NS-1, (e) NS-2 arrangement, (f) shading dispersion (SD) in NS-2. In Table 6, a comparison of TCT, NS-1, and NS-2 parameters is provided. Table 4 shows that ML for NS-1 and NS-2 is 11.9% and 11.58%, respectively. Whereas for total cross tied, it is 21.6463%. The NS-1 and NS-2 have FF of 67.7599% and 70.4352%, respectively, and for TCT is 58.137%. Under this shading condition, the power enhanced by NS-1 is 12.4143%, and NS-2 is 12.8126% compared to the TCT configuration. Figure 11 shows the power-voltage characteristic for BOLC shading for a 4 × 4 sub-array and uniform shading. This characteristic represents the P-V curve for TCT under normal shading condition, TCT under partial shading condition, NS-1, and NS-2 under shading conditions. From the PV curve. The results show that the NS-1 has the highest GMPP point under shading conditions, NS-2 is slightly lower than NS-1, and TCT has the lowest GMPP point under partial shading conditions.

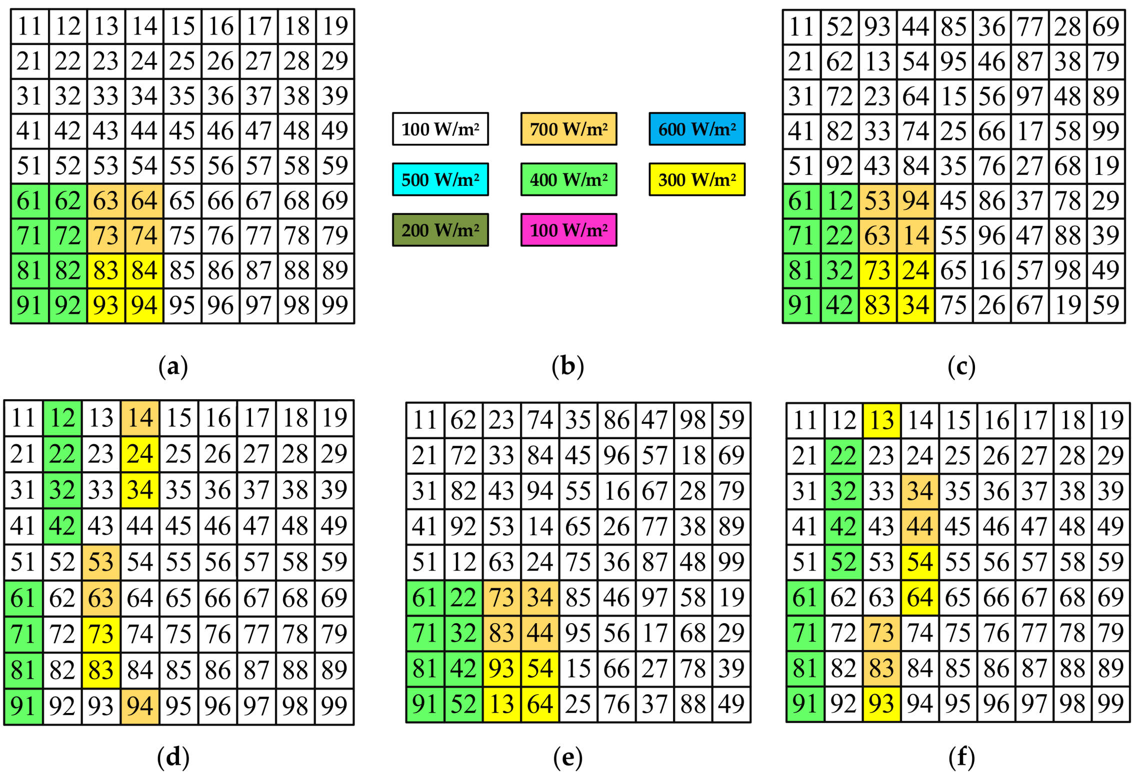

Figure 10. BOLC 4 × 4 subarray shading for a 9 × 9 array. (**a**) total cross tied arrangement, (**b**) solar insolation levels (SIL), (**c**) NS-1 arrangement, (**d**) shading dispersion (SD) in NS-1, (**e**) NS-2 arrangements, (**f**) shading dispersion (SD) in NS-2.

Table 6. Comparison between total cross tied, NS-1, and NS-2 arrangements under BOLC 4 × 4 sub-array shading condition.

Method	V_{oc} (Volts)	I_{sc} (Ampere)	GMPP (Watt)	I_{GMPP} (Ampere)	V_{GMPP} (Volts)	% Power Loss	% Fill Factor
TCT	395.5285	46.9407	10,794	31.6932	340.5731	21.6463	58.1370
NS1	395.6759	45.2576	12,134	37.5343	323.2727	11.9000	67.7599
NS2	395.6798	43.6925	12,177	37.4041	325.5426	11.5800	70.4352

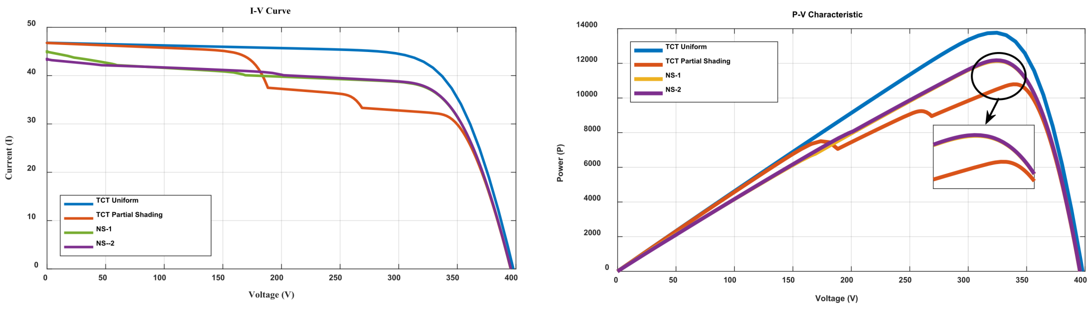

(**a**) (**b**)

Figure 11. (**a**) I-V curve and (**b**) P-V curve for BOLC 4 × 4 subarray and uniform shading.

4.4. Third: TORC 4 × 4 Sub-Array Shading Condition

TORC means Top of Right Corner 4 × 4 sub-array. In this shading effect, TCT, non-symmetrical-1, and non-symmetrical-2 were compared based on ML, FF, and η. Figure 12 shows the TORC 4 × 4 sub-array shading for (a) total cross tied arrangement, (b) solar insolation levels (SIL), (c) NS-1 arrangement, (d) shading dispersion (SD) in NS-1, (e) NS- 2 arrangements, (f) shading dispersion (SD) in NS-2. A comparison is presented in Table 7 of TCT, NS-1, and NS-2 parameters and it was observed that FF for NS-1 and NS-2 is 66.4455% and 66.3883%, respectively. Whereas for TCT, it is 54.5310%. The NS-1 and NS-2 have ML of 14.76% and 14.8333%, respectively, and for TCT it is 26.6550%. Under this shading condition, the power enhanced by NS-1 is 16.1916% and NS-2 is 16.09% compared to the TCT configuration. Figure 13 shows the power-voltage characteristic for TORC shading for a 4 × 4 sub-array and uniform shading condition. This characteristic represents the P-V curve for TCT under normal shading conditions, TCT under partial shading conditions, NS-1 and NS-2 under TORC shading conditions. The PV curve also observed that the NS-1 and NS-2 has nearly the same GMPP point under shading condition and followed by NS-2 and TCT under partial shading condition. The P-V curve for NS-1 and NS-2 is overlapping. The TCT under shading conditions has three power peaks, while NS- 1 and NS-2 reduce these multiple power peaks.

Table 7. Comparison between total cross tied, NS-1, and NS-2 arrangements under TORC 4 × 4 sub-array shading condition.

Method	V_{oc} (Volts)	I_{sc} (Ampere)	GMPP (Watt)	I_{GMPP} (Ampere)	V_{GMPP} (Volts)	% Power Loss	% Fill Factor
TCT	394.7300	46.9407	10,104	29.6743	340.4987	26.6550	54.5310
NS1	394.9547	44.7358	11,740	36.2547	323.8321	14.7600	66.4455
NS2	394.9578	44.7358	11,730	35.8959	326.7896	14.8333	66.3883

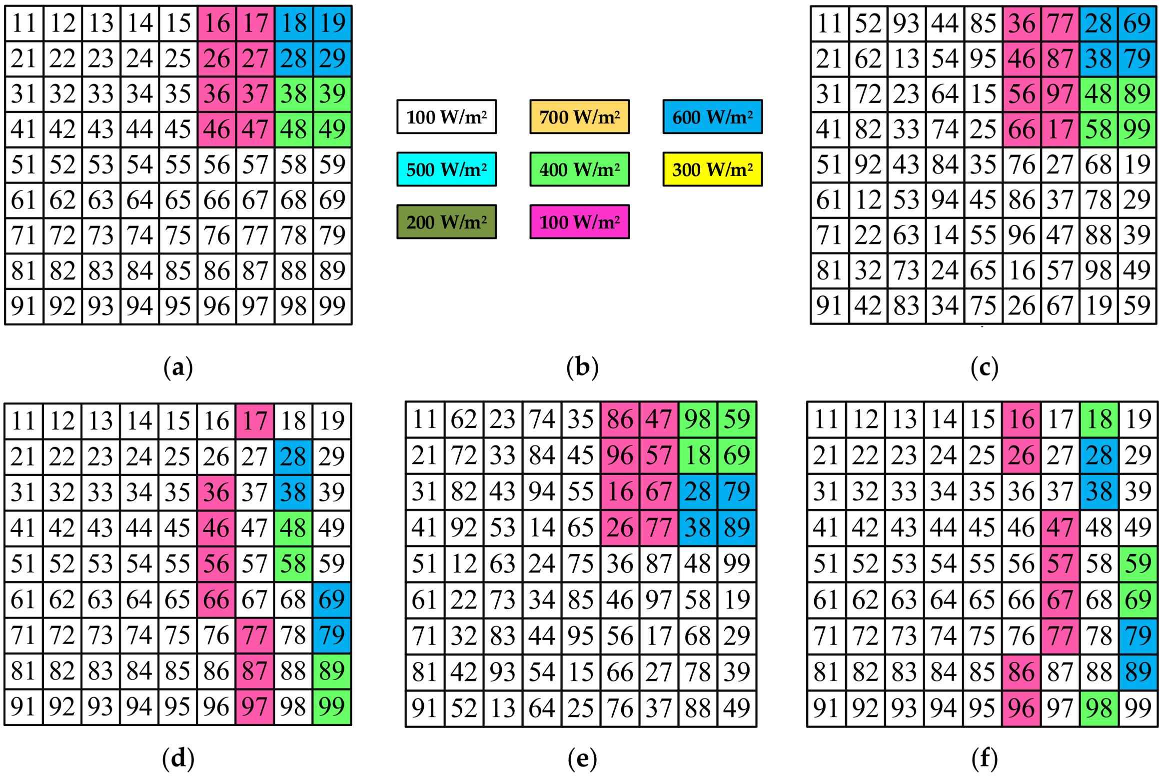

Figure 12. TORC 4 × 4 subarray shading for 9 × 9 array. (**a**) Total cross tied arrangement, (**b**) solar insolation levels (SIL), (**c**) NS-1 arrangement, (**d**) shading dispersion (SD) in NS-1, (**e**) NS-2 arrangement, (**f**) shading dispersion (SD) in NS-2.

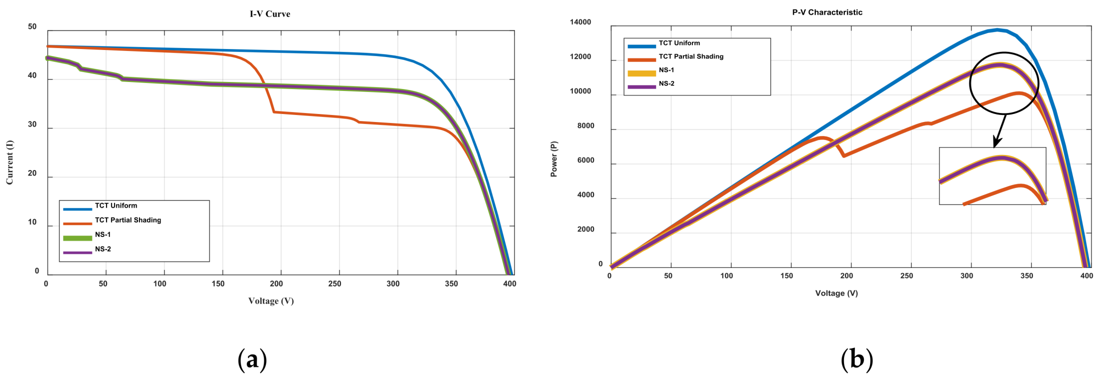

Figure 13. (**a**) I-V curve and (**b**) P-V curve for TORC 4 × 4 subarray and uniform shading.

4.5. Fourth: TOLC 4 × 4 Sub-Array Shading Condition

TOLC means Top of Left Corner 4 × 4 sub-array. In this shading effect, parameters were related between TCT, non-symmetrical-1, and non-symmetrical-2 based on ML, FF, and η. Figure 14 shows the TOLC 4 × 4 sub-array shading for (a) TCT arrangement, (b) solar insolation levels (SIL), (c) NS-1 arrangement, (d) shading dispersion (SD) in NS-1, (e) NS- 2 arrangement, (f) shading dispersion (SD) in NS-2. In Table 8, a comparison of TCT, NS-1, and NS-2 parameters is provided. It shows that FF for NS-1 and NS-2 is 66.7925% and 68.6418%, respectively. Whereas for total cross tied, it is 54.2228%. The NS-1 and NS-2 have ML of 15.3488% and 15.05%, respectively and for TCT is 27.0978%. Under this shading condition, the power enhanced by NS-1 is 16.0908% and NS-2 is 16.4890% compared to TCT configuration. Figure 15 shows the power-voltage characteristic for TOLC 4 × 4 Sub-Array and uniform shading condition. This characteristic represents the P-V curve for TCT under normal shading conditions, TCT under partial shading conditions, NS-1 and NS-2 under TORC shading conditions. The PV curve highlights that the NS-1 and NS-2 have nearly the same GMPP point under shading conditions, followed by NS-2 and TCT under considered PSC. The P-V curve for NS-1 and NS-2 is overlapping. The TCT under shading this condition has two different power peaks while NS-1 and NS-2 reduce the multiple power peaks.

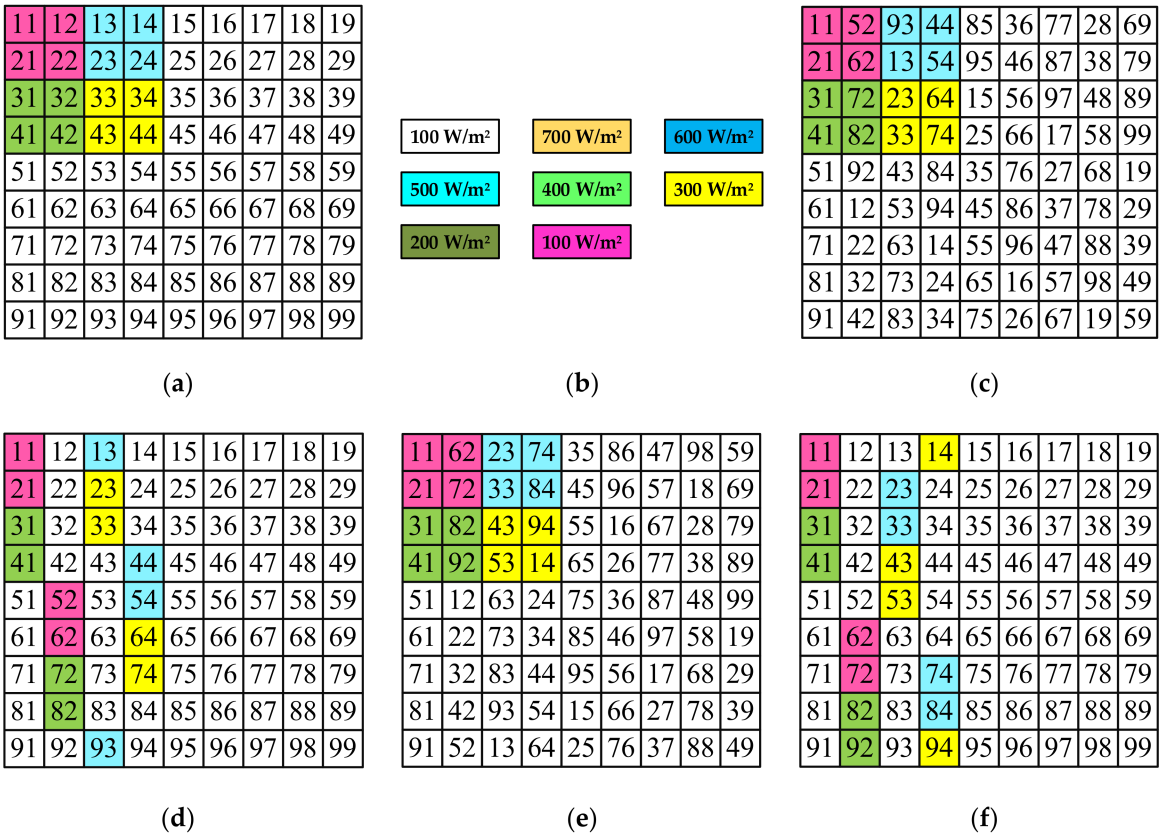

Figure 14. TORC 4 × 4 subarray shading for 9 × 9 array. (**a**) Total cross tied arrangement, (**b**) solar insolation levels (SIL). (**c**) NS-1 arrangement, (**d**) shading dispersion (SD) in NS-1, (**e**) NS-2 arrangement, (**f**) shading dispersion (SD) in NS-2.

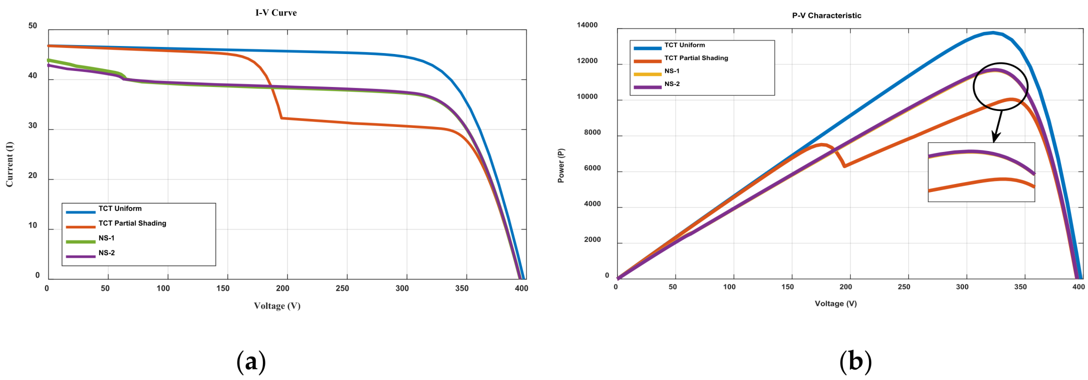

Figure 15. (**a**) I-V curve and (**b**) P-V curve for TOLC 4 × 4 subarray and uniform shading.

Table 8. Comparison between total cross tied, NS-1, and NS-2 arrangements under TOLC 4 × 4 sub-array shading condition.

Method	V_{oc} (Volts)	I_{sc} (Ampere)	GMPP (Watt)	I_{GMPP} (Ampere)	V_{GMPP} (Volts)	% Power Loss	% Fill Factor
TCT	394.5770	46.9407	10,043	29.7798	337.2400	27.0978	54.2228
NS1	394.7959	44.2141	11,659	35.9232	325.1889	15.3488	66.7925
NS2	394.7943	43.1707	11,699	36.0765	324.2842	15.0500	68.6418

4.6. Fifth: 4 × 4 Sub-Array Shading Condition at Center

In this 4 × 4 sub-array, the shading condition is located at the center. In this shading effect, total cross tied, non-symmetrical-1, and non-symmetrical-2 were compared based on various parameters such as ML, FF, and η. Figure 16 shows the center 4 × 4 sub-array shading for (a) total cross tied arrangement, (b) solar insolation levels (SIL), (c) NS-1 arrangement, (d) shading dispersion (SD) in NS-1 and (e) NS-2 arrangements, (f) shading dispersion (SD) in NS-2. In Table 9, a comparison of TCT, NS-1, and NS-2 parameters is presented.

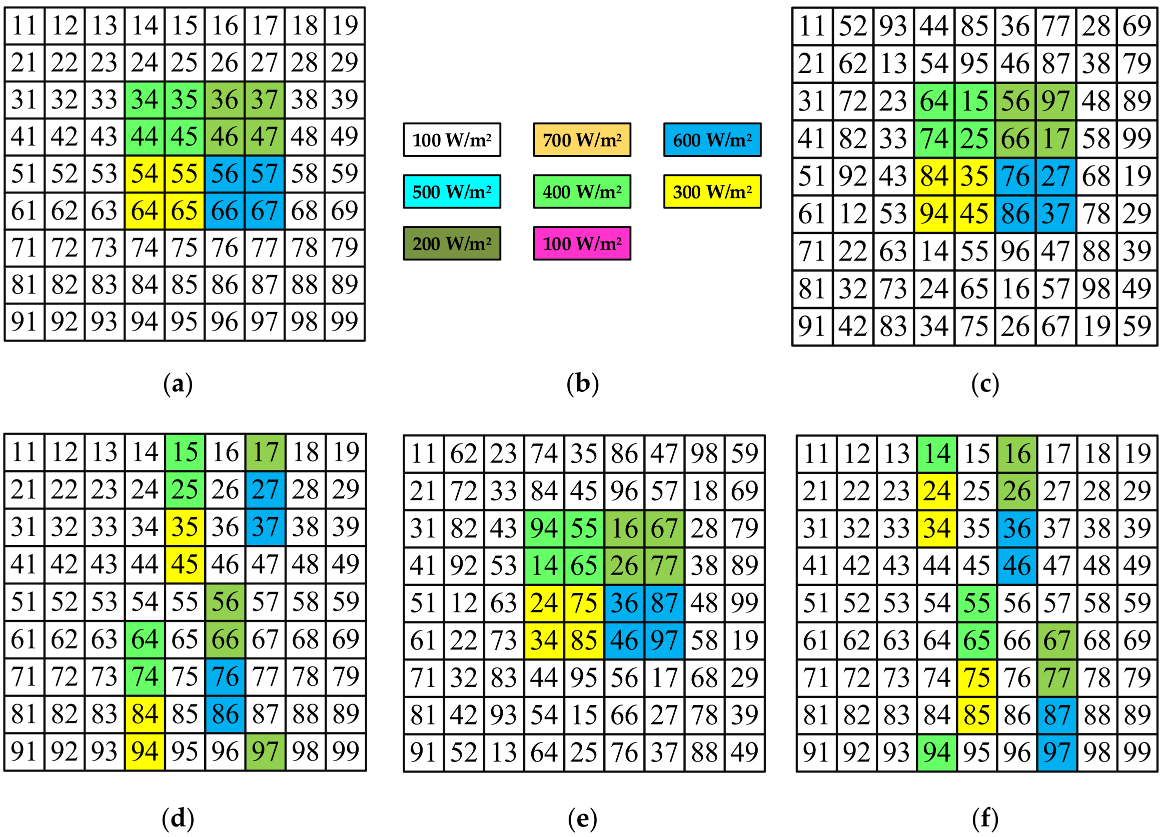

Figure 16. The 4 × 4 sub-array shading condition at center 9 × 9 array. (**a**) Total cross tied arrangement, (**b**) solar insolation levels (SIL), (**c**) NS-1 arrangement, (**d**) shading dispersion (SD) in NS-1, (**e**) NS-2 arrangement, (**f**) shading dispersion (SD) in NS-2.

Table 9. Comparison between total cross tied, NS-1, and NS-2 arrangements under 4 × 4 sub-array shading condition at the center.

V_{oc} (Volts)	I_{sc} (Ampere)	GMPP (Watt)	I_{GMPP} (Ampere)	V_{GMPP} (Volts)	% Power Loss	% Fill Factor
395.1000	46.9407	10,458	30.7980	339.5553	24.0854	56.3887
395.3085	43.1707	11,960	36.8704	324.3865	13.1634	70.0819
395.3257	44.7358	11,903	36.6855	324.4683	13.5772	67.3048

The same Table 9 shows that FF for NS-1 and NS-2 is 70.0819% and 67.3048%, respectively. Whereas for total cross tied, it is 56.3887%. The NS-1 and NS-2 have ML of 13.1634% and 13.5772%, respectively, and for total cross tied is 24.0854%. Under this shading condition, the power enhanced by NS-1 is 14.3622% and NS-2 is 13.8172% compared to the total cross tied configuration. Figure 17 shows the power-voltage characteristic for center shading for the 4 × 4 sub-array and uniform shading condition. This characteristic represents the P-V curve for TCT under normal shading condition, TCT under partial shading condition, NS-1 and NS-2 under center shading for 4 × 4 sub-array shading condition. PV displays that the NS-1 and NS-2 have similar GMPP points under shading conditions followed by NS-2 and TCT under partial shading conditions. The P-V curve for NS-1 and NS-2 is overlapping. The TCT under shading conditions has three power peaks, while NS-1 and NS-2 reduce these multiple power peaks.

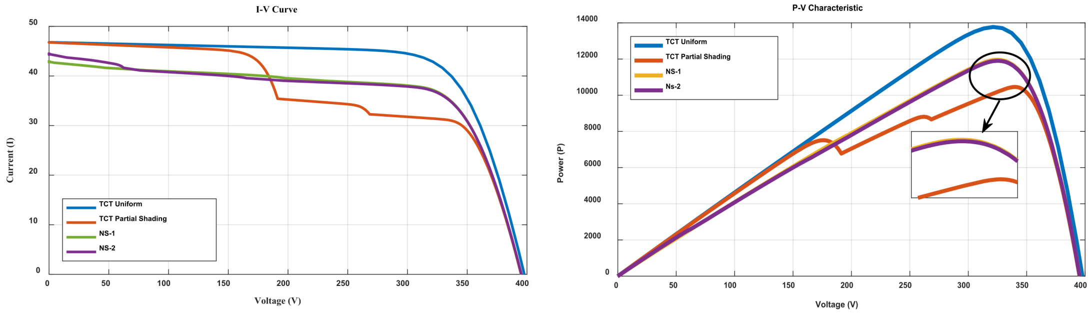

(**a**) (**b**)

Figure 17. (**a**) I-V curve and (**b**) P-V curve for 4 × 4 sub-array shading condition at the center and uniform shading.

4.7. Sixth: Two Sub-Arrays of 3 × 3 Shading Condition

This shading condition has two shaded sub-arrays of 3 × 3 size. Under this shading, ML, FF, and η were compared for total cross tied, non-symmetrical-1, and non-symmetrical-2. Figure 18 shows the two sub-arrays of 3 × 3 size shading. Table 10 provides the TCT, NS-1, and NS-2 parameters' comparison. Table 10 indicates that FF for NS-1 and NS-2 is 65.3225% and 65.3333%, respectively. Whereas for total cross tied it is 58.7683%. The NS-1 and NS-2 have ML of 16.1693% and 16.1765%, respectively, and for total cross tied it is 20.9349%. Table 11 reveals that the power enhanced by NS-1 is 6.0044% and NS-2 is 5.9952% compared to the total cross tied configuration. Figure 19 shows the power-voltage characteristic for two sub-arrays of 3 × 3 size shading and uniform shading conditions. This characteristic represents the P-V curve for TCT under normal shading condition, TCT under partial shading condition, NS-1 and NS-2 under center shading for the 4 × 4 sub-array shading condition. The PV curve shows that the NS-1 and NS-2 have nearly the same GMPP point this under shading condition, followed by NS-2 and TCT under partial shading conditions. The P-V curve for NS-1 and NS-2 is overlapping. The TCT under shading conditions has three power peaks, while NS-1 and NS-2 reduce these multiple power peaks.

Table 10. Comparison between total cross tied, NS-1, and NS-2 arrangements under two sub-arrays of 3 × 3 size shading condition.

Method	V_{oc} (Volts)	I_{sc} (Ampere)	GMPP (Watt)	I_{GMPP} (Ampere)	V_{GMPP} (Volts)	% Power Loss	% Fill Factor
TCT	395.0000	46.9210	10,892	32.5142	335.0006	20.9349	58.7683
NS1	395.1058	44.7358	11,546	34.8785	331.0442	16.1693	65.3225
NS2	395.0062	44.7358	11,545	34.9012	330.8230	16.1765	65.3333
Sixth	10,892	11,546	11,545	06.0044		5.99520	

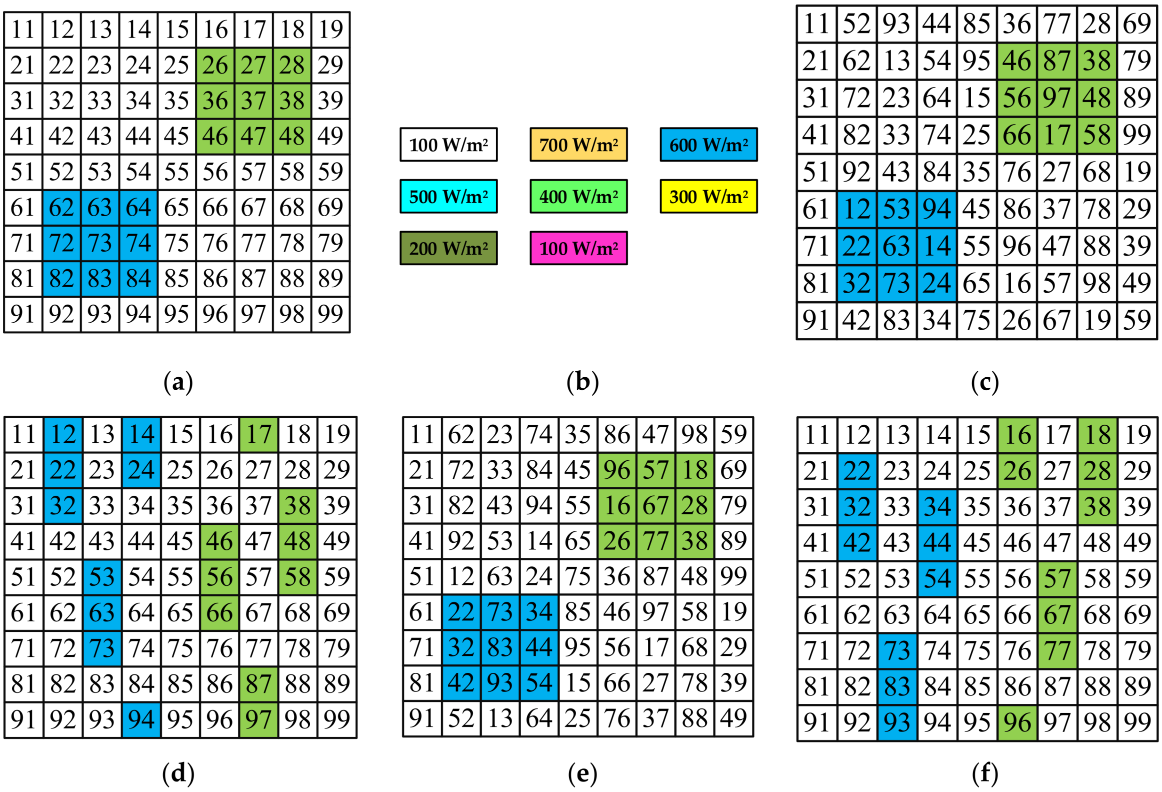

Figure 18. Two sub-arrays of 3 × 3 size shading condition in 9 × 9 array. (**a**) Total cross tied arrangement, (**b**) solar insolation levels (SIL), (**c**) NS-1 arrangement, (**d**) shading dispersion (SD) in NS-1, (**e**) NS-2 arrangement, (**f**) shading dispersion (SD) in NS-2.

Table 11. Comparison of TCT, NS-1, and NS-2 reconfiguration techniques based on GMPP, % power enhancement under shading types.

Shading Type	TCT P_{GMP} (in Watts)	NS-1 P_{GMP} (in Watts)	NS-2 P_{GMP} (in Watts)	% Power Enhanced in NS-1 Compared to TCT	% Power Enhanced in NS-2 Compared to TCT
First	11,605	12,696	12,486	09.4011	07.5900
Second	10,794	12,134	12,177	12.4143	12.8126
Third	10,104	11,740	11,730	16.1916	16.0900
Fourth	10,043	11,659	11,699	16.0908	16.4890
Fifth	10,458	11,960	11,903	14.3622	13.8172

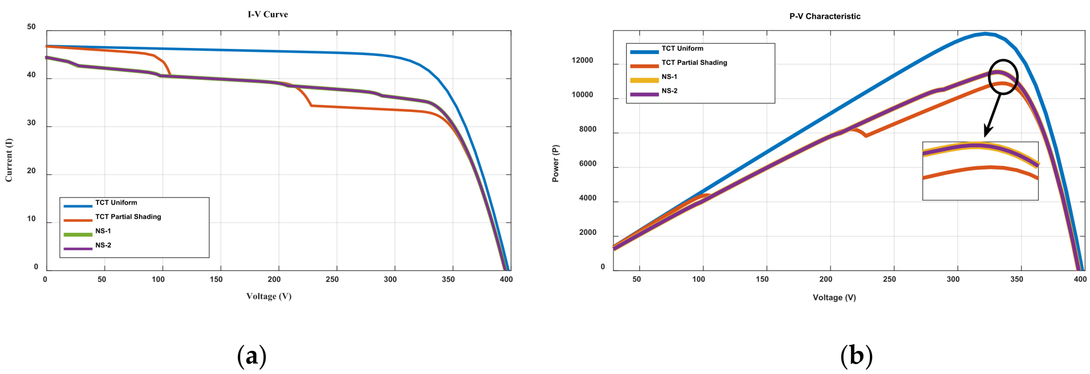

Figure 19. (**a**) I-V curve and (**b**) P-V curve for two sub-arrays of 3 × 3 size shading condition and uniform shading.

The fill factor is the ratio of the maximum power (GMPP = I_{GMPP} * V_{GMPP}) generated by a solar cell to the product of Voc and I_{SC}. FF depends on the Rs (series resistance) and Rsh (shunt resistance) and carrier recombination of the solar cell. In a solar cell, the ideality factor measures the junction quality and type of recombination. The impact of shunt resistance, when recombination current dominates in the junction, causes the ideality factor value to be greater than one for low bias voltages or low currents. Low Voc is also a result of high recombination. Under partial shading conditions, there is a decrease in fill factor and power maximums due to a reduction in the photocurrent and photo voltage. The performance of FF is visually depicted in Figures 20–25 for the six considered shading situations. Tables 3–8 summarize the equivalent FF and % power loss values under the shading effect. Furthermore, it concludes that the FF performs better in reconfigurations than TCT. Figure 26 shows the P_{GMP} (in watts) for various shading conditions. The output of solar PV is not constant, and it is a function of time and solar insolation. This article compares conventional configuration and reconfiguration techniques based on MATLAB simulation results and calculation. Under all above-mentioned partial shading conditions, the P_{GMP} (in watts) of discussed methods and their power enhancement comparison are values are mentioned in Table 11.

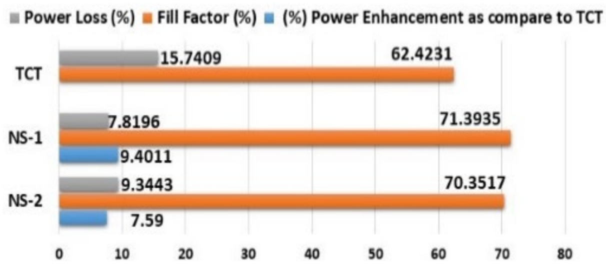

Figure 20. The first shading condition.

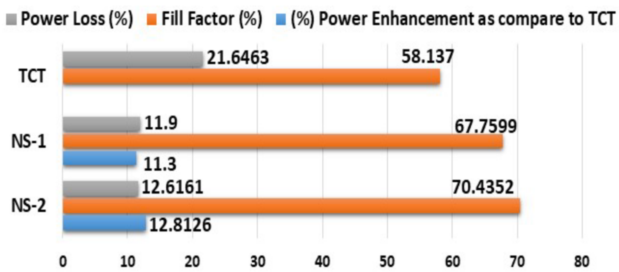

Figure 21. The second shading condition.

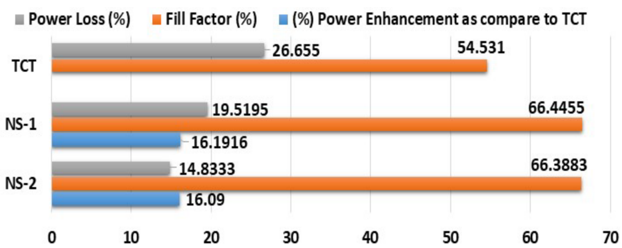

Figure 22. The third shading condition.

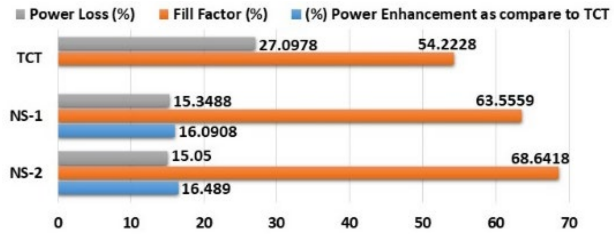

Figure 23. The fourth shading condition.

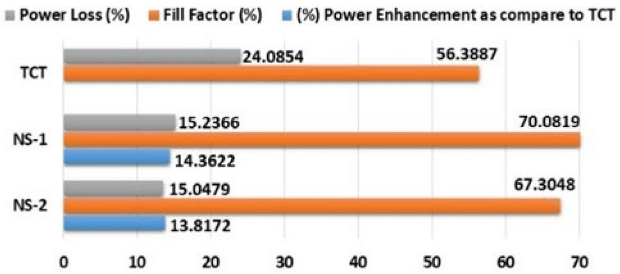

Figure 24. The fifth shading condition.

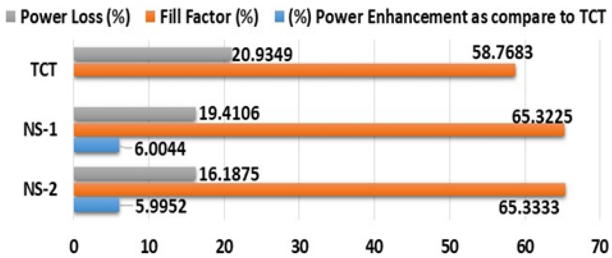

Figure 25. The sixth shading condition.

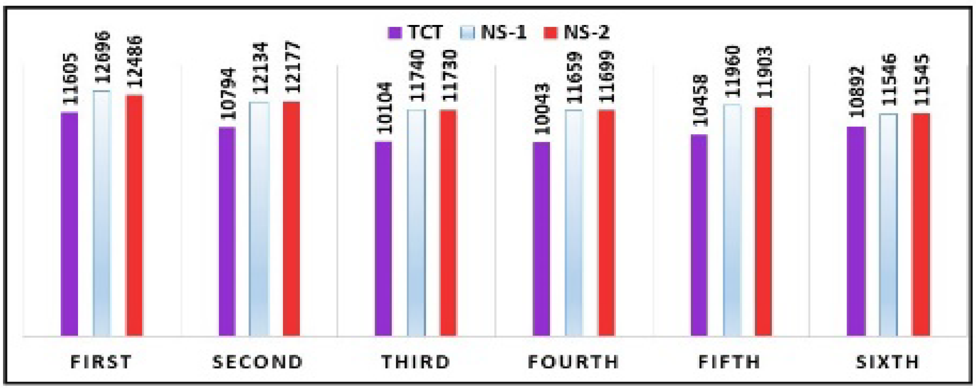

Figure 26. P_{GMP} for different shading conditions.

In the first shading condition, the P_{GMP} (in watts) value for TCT is 11,605, for NS-1 and NS-2 is 12,696 and 12,486. In the second shading condition, the P_{GMP} (in watts) value for TCT is 10,794, and for NS-1 and NS-2 is 12,134 and 12,177. In the third shading condition, the P_{GMP} (in watts) value for TCT is 10,104 and for NS-1 and NS-2 is 11,740 and 11,730. In the fourth shading condition, the P_{GMP} (in watts) value for TCT is 11,605 and for NS-1 and NS-2 is 11,659 and 11,699. In the fifth shading condition, the value of P_{GMP} (in watts) TCT is 10,458 and NS-1 and NS-2 are 11,960 and 11,903. In the sixth shading condition, the P_{GMP} (in watts) value for TCT is 10,892 and for NS-1 and NS-2 is 11,546 and 11,545.

5. Conclusions

The simulation results conclude that both NS-1 and NS-2 methods enhance the power generation capability under all the considered partial shading conditions. Under 50% shading cases, NS-1 gives the highest % PE, while NS-2 does for the rest of the shading conditions. Utilizing non-symmetrical reconfiguration techniques for solar PV array helps to minimize power loss by 4% to 12% depending on PSC. The non-symmetrical reconfiguration technique reduces the power loss due to the shadow falling on PV. Under various PSC, TCT had a % FF between 54 and 62. Through non-symmetrical reconfiguration, it is enhanced up to 65–70%. Therefore, it can be concluded that the non-symmetrical reconfiguration technique provides good performance compared to the TCT configuration under shading effects.

6. PV Module Used

In this research paper, all the reconfiguration techniques are implemented by considering parameters shown in Table 12.

Table 12. PV module used.

Parameter	Ratings
Power	170 W
V_{OC}	44.2 V
I_{SC}	5.2 A
V_{MP}	35.8 V
I_{MP}	4.75 A
Number of cells	72

Author Contributions: Conceptualization, methodology, Investigation, resources, data curation, visualization, writing—original draft preparation—S.M. and A.K.; software validation, formal analysis, writing—review and editing—S.M., A.K., P.K.B., T.S.; supervision, project administration, Funding acquisition—S.M. and T.S. All authors have read and agreed to the published version of the manuscript.

Funding: The authors gratefully acknowledge the support offered by the Science and Engineering Research Board (SERB), Department of Science and Technology (DST), Government of India under the grant number EEQ/2021/00294 for this research work.

Institutional Review Board Statement: Not Applicable.

Informed Consent Statement: Not Applicable.

Data Availability Statement: Not Applicable.

Conflicts of Interest: The authors declare no conflict of interest.

References

1. Hachim, B.; Dahlioui, D.; Barhdadi, A. Electrification of rural and arid areas by solar energy applications case study: Boumhaout village in south of Morocco. In Proceedings of the 2018 6th International Renewable and Sustainable Energy Conference, IRSEC 2018, Rabat, Morocco, 5–8 December 2018; Volume 1, pp. 1–4. [CrossRef]
2. Choudhary, S. Global Energy Demand to Increase by 4.6% in 2021. 2020, pp. 11–12. Available online: https://economictimes.indiatimes.com/industry/energy/oil-gas/global-energy-demand-to-increase-by-4-6-in-2021-iea/articleshow/82163196.cms (accessed on 8 December 2021).
3. Radhakrishnan, V. October Saw Highest Power Shortage in over 5 Years. 2021. Available online: https://www.thehindu.com/news/national/october-2021-saw-highest-power-shortage-in-over-5-years/article37361732.ece#:~{}:text=In%20October%2C%20Gujarat%20recorded%20a,in%20more%20than%20a%20decade (accessed on 28 November 2021).
4. Negi, A.; Kumar, A. Long-term Electricity Demand Scenarios for India: Implications of Energy Efficiency. In Proceedings of the 2018 International Conference on Power Energy, Environment and Intelligent Control, PEEIC 2018, Greater Noida, India, 13–14 April 2018; pp. 462–467. [CrossRef]

5. Meral, M.E.; Diner, F. A review of the factors affecting operation and efficiency of photovoltaic based electricity generation systems. *Renew. Sustain. Energy Rev.* **2011**, *15*, 2176–2184. [CrossRef]
6. Jordehi, A.R. Maximum power point tracking in photovoltaic (PV) systems: A review of different approaches. *Renew. Sustain. Energy Rev.* **2016**, *65*, 1127–1138. [CrossRef]
7. Chandrakant, C.V.; Mikkili, S. A typical review on static reconfiguration strategies in photovoltaic array under non-uniform shading conditions. *CSEE J. Power Energy Syst.* **2020**, 1–33. [CrossRef]
8. Boddapati, V.; Sree, A.; Nandikatti, R. Energy for Sustainable Development Salient features of the national power grid and its management during an emergency: A case study in India. *Energy Sustain. Dev.* **2020**, *59*, 170–179. [CrossRef]
9. Kumar, N.; Tripathi, M.M. Solar Power Trading Models for Restructured Electricity Market in India. *Asian J. Water Environ. Pollut.* **2020**, *17*, 49–54. [CrossRef]
10. Purohit, I.; Purohit, P. Performance assessment of grid-interactive solar photovoltaic projects under India' s national solar mission. *Appl. Energy* **2018**, *222*, 25–41. [CrossRef]
11. Wang, Y.; Das, R.; Putrus, G.; Kotter, R. Economic evaluation of photovoltaic and energy storage technologies for future domestic energy systems—A case study of the UK. *Energy* **2020**, *203*, 117826. [CrossRef]
12. Christabel, S.C.; Srinivasan, A.; Winston, D.P.; Kumar, B.P. Reconfiguration solution for extracting maximum power in the aged solar PV systems. *J. Electr. Eng.* **2016**, *16*, 440–446.
13. Braun, H.; Buddha, S.T.; Krishnan, V.; Tepedelenlioglu, C.; Spanias, A.; Banavar, M.; Srinivasan, D. Topology reconfiguration for optimization of photovoltaic array output. *Sustain. Energy Grids Netw.* **2016**, *6*, 58–69. [CrossRef]
14. Agarwal, N.; Agarwal, A. Mismatch Losses in Solar Photovoltaic Array. *MIT Int. J. Electr. Instrum. Eng.* **2014**, *4*, 16–19.
15. Horoufiany, M.; Ghandehari, R. Optimal fixed reconfiguration scheme for PV arrays power enhancement under mutual shading conditions. *IET Renew. Power Gener.* **2017**, *11*, 1456–1463. [CrossRef]
16. Postovoit, B.; Susoeff, D.; Daghbas, D.; Holt, J.; Pomona, C.P.; Le, H.T. A Solar-Based Stand-Alone Family House for Energy Independence and Efficiency. In Proceedings of the 2020 IEEE Conference on Technologies for Sustainability, SusTech 2020, Santa Ana, CA, USA, 23–25 April 2020. [CrossRef]
17. Chavan, V.C.; Mikkili, S. Effect of PV Array Positioning on Mismatch and Wiring Losses in Static Array Reconfiguration. *IETE J. Res.* **2021**, 1–14. [CrossRef]
18. Pendem, S.R.; Mikkili, S. Modeling, simulation, and performance analysis of PV array configurations (Series, Series-Parallel, Bridge-Linked, and Honey-Comb) to harvest maximum power under various Partial Shading Conditions. *Int. J. Green Energy* **2018**, *15*, 795–812. [CrossRef]
19. Manjunath Suresh, H.N.; Rajanna, S. Performance enhancement of Hybrid interconnected Solar Photovoltaic array using shade dispersion Magic Square Puzzle Pattern technique under partial shading conditions. *Sol. Energy* **2019**, *194*, 602–617. [CrossRef]
20. Kumar, B.P.; Cherukuri, S.K.; Kaniganti, K.R.; Karuppiah, N.; Muniraj, R. Performance Enhancement of Partial Shaded Photovoltaic System With the Novel Screw Pattern Array Configuration Scheme. *IEEE Access* **2022**, *10*, 1731–1744. [CrossRef]
21. Bonthagorla, P.K.; Mikkili, S. A Novel Fixed PV Array Configuration for Harvesting Maximum Power from Shaded Modules by Reducing the Number of Cross-Ties. *IEEE J. Emerg. Sel. Top. Power Electron.* **2020**, *9*, 2109–2121. [CrossRef]
22. Ajmal, A.M.; Sudhakar Babu, T.; Ramachandaramurthy, V.K.; Yousri, D.; Ekanayake, J.B. Static and dynamic reconfiguration approaches for mitigation of partial shading influence in photovoltaic arrays. *Sustain. Energy Technol. Assess.* **2020**, *40*, 100738. [CrossRef]
23. Pachauri, R.K.; Alhelou, H.H.; Bai, J.; Golshan, M.E.H. Adaptive Switch Matrix for PV Module Connections to Avoid Permanent Cross-Tied Link in PV Array System under Non-Uniform Irradiations. *IEEE Access* **2021**, *9*, 45978–45992. [CrossRef]
24. Ngo, T.; Nguyen, Q.; Nguyen, L.; Riva, E.; Romano, P.; Viola, F. Increasing efficiency of photovoltaic systems under non-homogeneous solar irradiation using improved Dynamic Programming methods. *Sol. Energy* **2017**, *150*, 325–334. [CrossRef]
25. Srinivasan, A.; Devakirubakaran, S. L-Shape Propagated Array Configuration With Dynamic Reconfiguration Algorithm for Enhancing Energy Conversion Rate of Partial Shaded Photovoltaic Systems. *IEEE Access* **2021**, *9*, 97661–97674. [CrossRef]
26. Malathy, S.; Ramaprabha, R. Reconfiguration strategies to extract maximum power from photovoltaic array under partially shaded conditions. *Renew. Sustain. Energy Rev.* **2018**, *81*, 2922–2934. [CrossRef]
27. Chavan, V.C.; Mikkili, S. Repositioning of Series-Parallel, Total-Cross-Tide, Bridge-Link, and Honey-Comb PV Array Configurations for Maximum Power Extraction. *IETE J. Res.* **2021**, 1–13. [CrossRef]
28. Rani, B.I.; Ilango, G.S.; Nagamani, C. Enhanced power generation from PV array under partial shading conditions by shade dispersion using Su Do Ku configuration. *IEEE Trans. Sustain. Energy* **2013**, *4*, 594–601. [CrossRef]
29. Sai Krishna, G.; Moger, T. Improved SuDoKu reconfiguration technique for total-cross-tied PV array to enhance maximum power under partial shading conditions. *Renew. Sustain. Energy Rev.* **2019**, *109*, 333–348. [CrossRef]
30. El Iysaouy, L.; Lahbabi, M.; Oumnad, A. A novel magic square view topology of a PV system under partial shading condition. *Energy Procedia* **2019**, *157*, 1182–1190. [CrossRef]
31. Sreekantha Reddy, S.; Yammani, C. A novel Magic-Square puzzle based one-time PV reconfiguration technique to mitigate mismatch power loss under various partial shading conditions. *Optik* **2020**, *222*, 165289. [CrossRef]

32. Nihanth, M.S.S.; Ram, J.P.; Pillai, D.S.; Ghias, A.M.; Garg, A.; Rajasekar, N. Enhanced power production in PV arrays using a new skyscraper puzzle based one-time reconfiguration procedure under partial shade conditions (PSCs). *Sol. Energy* **2019**, *194*, 209–224. [CrossRef]
33. Pillai, D.S.; Rajasekar, N.; Ram, J.P.; Chinnaiyan, V.K. Design and testing of two phase array reconfiguration procedure for maximizing power in solar PV systems under partial shade conditions (PSC). *Energy Convers. Manag.* **2018**, *178*, 92–110. [CrossRef]